

Effects of sphingomyelin on melittin pore formation

María J. Gómara^a, Shlomo Nir^b, José L. Nieva^{a,*}

^aUnidad de Biofísica (CSIC-UPV/EHU) and Departamento de Bioquímica, Universidad del País Vasco, Aptdo. 644, 48080 Bilbao, Spain

^bSeagram Center for Soil and Water Sciences, Faculty of Agricultural, Food and Environmental Quality Sciences, The Hebrew University of Jerusalem, Rehovot 76100, Israel

Received 11 December 2002; accepted 19 March 2003

Abstract

The effect of sphingomyelin (SM), one of the main lipids in the external monolayer of erythrocyte plasma membrane, on the ability of the hemolytic peptide melittin to permeabilize liposomes was investigated. The peptide induced contents efflux in large unilamellar vesicles (LUV) composed of 1-palmitoyl-2-oleoylphosphatidylcholine (POPC)/SM (1:1 mole ratio), at lower ($>1:10,000$) peptide-to-lipid mole ratios than in pure POPC ($>1:1000$) or POPC/1-palmitoyl-2-oleoylphosphatidylglycerol (POPG) (1:1 mole ratio) ($>1:300$) vesicles. Analysis of the leakage data according to a kinetic model of pore formation showed a good fit for hexameric–octameric pores in SM-containing vesicles, whereas mediocre fits and lower surface aggregation constants were obtained in POPC and POPC/POPG vesicles. Disturbance of lateral separation into solid (s_o) and liquid-disordered (l_d) phases in POPC/SM mixtures increased the peptide-dose requirements for leakage. Inclusion of cholesterol (Chol) in POPC/SM mixtures under conditions inducing lateral separation of lipids into liquid-ordered (l_o) and l_d phases did not alter the number of melittin peptides required to permeabilize a single vesicle, but increased surface aggregation reversibility. Partitioning into liposomes or insertion into lipid monolayers was not affected by the presence of SM, suggesting that: (i) melittin accumulated at comparable doses in membranes with different SM content, and (ii) differences in leakage were due to promotion of melittin transmembrane pores under coexistence of s_o – l_d and l_o – l_d phases. Our results support the notion that SM may regulate the stability of size-defined melittin pores in natural membranes.

© 2003 Elsevier Science B.V. All rights reserved.

Keywords: Melittin; Lytic peptide; Membrane pore; Peptide–lipid interaction; Lipid domain; Cholesterol; Sphingolipid

1. Introduction

Melittin, the main peptide isolate from honey bee venom, is highly hemolytic and has been shown to enhance permeability of biomembranes (for a review, see Ref. [1]). It is generally assumed that direct interaction of melittin with lipids is required for its membrane-lytic activity. Current understanding of the melittin-induced membrane perturba-

tion mechanisms has led to mutually nonexclusive, alternative proposals for explaining its mode of action. Regardless of the lipid composition, at low membrane loads, amphipathic helical peptide monomers accumulate at membrane interfaces arranged parallel to the bilayer plane (Ref. [2] and references therein). The increase in surface concentrations of the peptide has been proposed to induce the formation of lytic pores consisting of transmembrane helices in a barrel-stave arrangement [3–5]. Helix translocation across membranes and assembly of size-defined permeating pores would be particularly favored in electrically neutral lipid bilayers. Alternatively, due to its cationic character, the peptide seems to remain tightly bound to the interface of negatively charged membranes [5,6]. Asymmetric accumulation of surface-bound peptides into one monolayer causes nonselective bilayer damage most likely according to a “detergent-like” or “carpet-like” [5] mechanism. Yet another membrane-disrupting mechanism has been described to occur at high melittin concentrations in solid phase (s_o) bilayers [7–9].

Abbreviations: ANTS, 8-aminonaphthalene-1,3,6-trisulfonic acid sodium salt; Chol, cholesterol; DMSO, dimethylsulfoxide; DPX, *p*-xylenebis(pyridinium)bromide; l_o , liquid-ordered; l_d , liquid-disordered; LUV, large unilamellar vesicles; PC, phosphatidylcholine; POPC, 1-palmitoyl-2-oleoylphosphatidylcholine; POPG, 1-palmitoyl-2-oleoylphosphatidylglycerol; s_o , solid; SM, sphingomyelin; T_m , melting temperature

* Corresponding author. Departamento de Bioquímica, Universidad del País Vasco, Aptdo. 644, 48080 Bilbao, Spain. Tel.: +34-94-6013353; fax: +34-94-4643360.

E-mail address: gbpniesj@lg.ehu.es (J.L. Nieva).

These membranes are fragmented giving rise to micellar particles or discs, with lipids in a bilayer organization surrounded with peptide molecules that protect hydrophobic edges from interaction with aqueous solution.

Kinetics and final extents of leakage induced by several peptides could be explained and predicted in the framework of a mathematical model of pore formation (reviewed in Ref. [10]). The model assumes that: (1) following a rapid stage of peptide binding to the vesicle membranes, surface aggregation of peptide occurs, and (2) when the structure and conformation of the peptides used are appropriate, the aggregates that have reached a critical size, that is, include M or more peptides, will form a pore. If surface aggregation of the peptide is irreversible, then vesicles that include M or more bound peptides will eventually leak all their encapsulated contents, whereas the other vesicles will not leak at all. The kinetics of leakage is dictated by the kinetics of surface aggregation, since once a pore has formed, the leakage of all the contents occurs within less than 1 s [11], thus yielding a finite final extent. When surface aggregation is reversible, only a fraction of the vesicles containing more than M peptides will include a pore and consequently leak all their contents.

We apply here such an analysis to describe the effects of sphingomyelin (SM) on the formation of melittin pores in large unilamellar vesicles (LUV). Although SM and phosphatidylcholine (PC) contain identical phosphocholine polar head-groups, they strongly differ in their physicochemical properties. In particular, natural SM is known to induce lateral segregation of lipids into enriched domains and to form specific complexes with cholesterol (Chol) [12–14], properties not shared by the natural PC. Our data indicate that under conditions required for coexistence of ordered and disordered lipid phases, SM promotes melittin pore assembly. Pore formation efficiency diminishes in the presence of Chol due to an increase in surface aggregation reversibility. Collectively, these findings contribute to sustain the notion that lipid composition may be involved in modulating melittin toxin activity in natural membranes.

2. Materials and methods

Chol, 1-palmitoyl-2-oleoylphosphatidylcholine (POPC), 1-palmitoyl-2-oleoylphosphatidylglycerol (POPG) and SM were purchased from Avanti Polar Lipids (Birmingham, AL, USA). 8-Aminonaphthalene-1,3,6-trisulfonic acid sodium salt (ANTS) and *p*-xylenebis(pyridinium)bromide (DPX) were from Molecular Probes (Junction City, OR, USA). *N*-Oleoyl SM, *N*-acetyl-L-tryptophanamide (NATA) and Triton X-100 were obtained from Sigma (St. Louis, MO, USA). All other reagents were of analytical grade. Synthetic melittin was from Bachem (Bubendorf, Switzerland). Peptide stock solutions were prepared in dimethylsulfoxide (DMSO) (spectroscopy grade).

2.1. Preparation of vesicles

LUV were prepared following the extrusion method of Hope et al. [15] in 5 mM HEPES, 100 mM NaCl (pH 7.4) buffer. Lipid concentrations of liposome suspensions were determined by phosphate analysis [16]. Distribution of vesicle sizes was estimated by quasielastic light scattering using a Malvern Zeta-Sizer instrument.

2.2. Leakage assay

Release of vesicular contents to the medium was monitored by the ANTS/DPX assay [17]. LUV containing 12.5 mM ANTS, 45 mM DPX, 20 mM NaCl and 5 mM HEPES were obtained by separating the unencapsulated material by gel filtration in a Sephadex G-75 column eluted with 5 mM HEPES, 100 mM NaCl (pH 7.4). Osmolarities were adjusted to 200 mosM in a cryoscopic osmometer (Osmomat 030, Gonotec, Berlin, Germany). Fluorescence measurements were performed by setting ANTS emission at 520 nm and excitation at 355 nm. A cutoff filter (470 nm) was placed between the sample and the emission monochromator. The 0% leakage corresponded to the fluorescence of the vesicles at time zero; 100% leakage was the fluorescence value obtained after addition of Triton X-100 (0.5%, v/v).

2.3. Analysis of leakage via pore formation

The model assumes that the peptides added into a vesicle suspension bind, become incorporated within the bilayer, and aggregate. When an aggregate within a membrane has reached a critical size, that is, it consists of M peptides, a pore can be created within the membrane, and leakage of encapsulated molecules can occur. It is assumed that the process of peptide binding is rapid and once a pore has been formed in a vesicle, all its contents will leak quickly. Thus, this leakage must be characterized by an all or none mechanism, that is, the population of vesicles consists of those that did not leak at all, and those who leaked all of their contents. Furthermore, the leakage must terminate after a certain period to yield final extents, which depend on peptide-to-lipid ratios. The rate and extent of leakage are assumed to be limited by the rate and extent of formation of surface aggregates of M or more peptides. The number M and geometrical considerations dictate the upper size of leaking molecules [11]. In most of the cases, the surface aggregation of the peptides is not irreversible and depends on $K_s = C/D$, in which C and D denote on and off rate constants of surface aggregation [18,19].

In the current study, we focus on simulating the final extents of leakage induced by melittin. The above pore model may be suited for this analysis because: (1) melittin does not redistribute between vesicles [6]; (2) melittin-induced leakage obeys an all-or-none mechanism [6]; and (3) leakage depends on the size of the encapsulated compounds [4,5]. The calculations, which employ the param-

ters M (pore size) and K_s , degree of surface reversibility, use as input the partitioning of the peptide and size distribution of vesicles [18,20]. The calculations simulate the final extents of leakage as a function of peptide-to-lipid mole ratios.

2.4. Monolayer penetration

Surface pressure was determined in a fixed-area circular through (μ Trough S system, Kibron, Helsinki). Measurements were carried out at room temperature and under constant stirring. The aqueous phase consisted of 1 ml 5 mM HEPES, 100 mM NaCl (pH 7.4). Lipid mixtures, dissolved in chloroform, were spread over the surface and the desired initial surface pressure (π_0) was attained by changing the amount of lipid applied to the air–water interface. Peptide was injected into the subphase with a Hamilton microsyringe. At the concentrations used, the peptide alone induced negligible increase in surface pressure at the air–water interface.

3. Results

The first step of the melittin-induced hemolysis process involves the partitioning of the peptide into the external leaflet of the erythrocyte membrane. This membrane monolayer is particularly enriched in SM. Consequently, we decided to investigate whether this phospholipid might regulate melittin-induced release of trapped dye from LUV. In Fig. 1, we compare the ability of melittin to induce leakage from POPC, POPC/SM (1:1, mole ratio) and POPC/POPG (1:1, mole ratio) LUV. At the fixed 1:500 peptide-to-lipid mole ratio, melittin induced leakage more readily in POPC/SM vesicles than in pure POPC (panel A). The presence of negatively charged lipids is known to inhibit the lytic power of melittin [5,6]. Accordingly, the lowest level of leakage was observed for POPC/POPG LUV. Also in agreement with calcein-release data previously reported by Benachir and Lafleur [6], melittin induced ANTS leakage from POPC and POPC/POPG LUV at peptide-to-lipid mole ratios higher than ca. 1:1000 and 1:300, respectively (Fig. 1B), whereas maximum extents were observed at ratios of roughly 1:100 (POPC) and 1:10 (POPC/POPG). Inclusion of the zwitterionic SM in the vesicle composition does not alter its net electrical charge. However, the peptide-to-lipid ratio required for leakage decreased to approximately 1:10,000, while maximum extents were already obtained at 1:1000. Thus, the melittin dose required to permeabilize POPC/SM LUV was about one and two orders of magnitude lower than those required to permeabilize POPC and POPC/POPG LUV, respectively.

Previous analyses had indicated that melittin-induced leakage of LUV made of zwitterionic lipid occurs via pore formation [4–6]. Thus, we analyzed the data in Fig. 1B according to a mathematical pore model (see Section 2). For

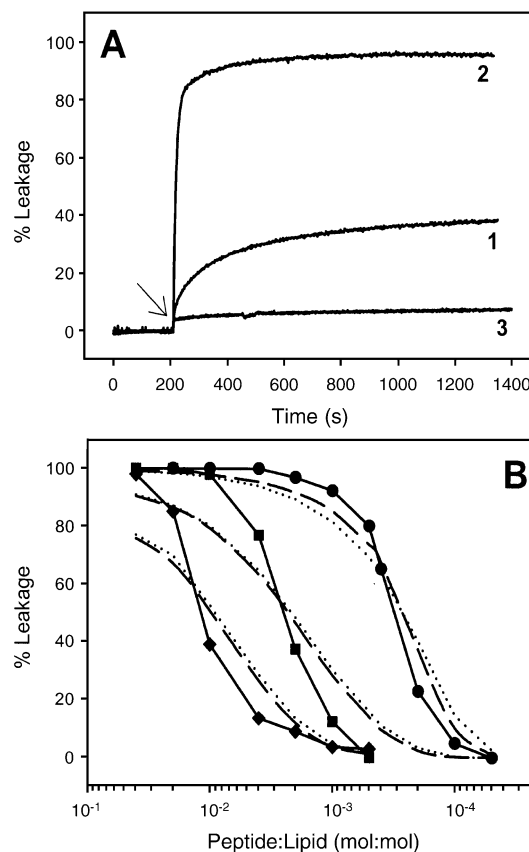


Fig. 1. Effects of SM and POPG on melittin-induced LUV permeabilization. (A) Kinetics of leakage following peptide addition (indicated by the arrow). 1: POPC; 2: POPC/SM (1:1); 3: POPC/POPG (1:1). In all samples, the added peptide-to-lipid ratio was 1:500 and lipid concentration was 100 μ M. (B) Final extents of leakage (percentage after 30 min) in POPC (squares), POPC/SM (1:1) (circles) and POPC/POPG (1:1) (diamonds) as a function of peptide-to-lipid mole ratio. Lipid concentration was 100 μ M. The curves correspond to the predicted values according to a pore model, calculated for $M=6$ (dashed) or $M=8$ (dotted).

melittin-induced leakage of POPC/SM (1:1) vesicles, final extents of leakage as a function of the peptide dose could be optimally fitted to hexameric ($M=6$) and octameric ($M=8$) pore models (R^2 of 0.95 and 0.97, respectively). Surface aggregation constant (K_s) values of 0.2 and 0.5 were obtained for $M=6$ and $M=8$, respectively, indicating a low degree of reversibility of melittin surface aggregation in this system (see also Table 1). By comparison, analysis of leakage from POPC vesicles yielded K_s values of 0.02 ($M=6$) and 0.03 ($M=8$), respectively, which implies a much higher level of reversibility of surface aggregation of the peptide. In this case, the experimental points could be fairly fitted to hexamer–octamer models ($R^2=0.93$ for both models). Finally, the experimental values obtained in negatively charged POPC/POPG (1:1) vesicles could be less successfully fitted to hexamer–octamer pore models (R^2 of 0.91 for both M values), whereas K_s values (0.002 and 0.004) suggested a high degree of surface aggregation reversibility in this system.

Table 1

Summary of calculations to obtain the best fits of final extents of ANTS/DPX leakage induced by melittin in different lipid mixtures

Lipid composition	M	K_s	R^2
POPC/POPG (1:1)	6	0.002	0.91
	8	0.004	0.91
POPC	6	0.020	0.93
	8	0.035	0.93
POPC/SM (4:1)	6	0.030	0.93
	8	0.050	0.93
POPC/SM (2:1)	6	0.045	0.91
	8	0.090	0.91
POPC/SM (1:1)	6	0.200	0.95
	8	0.500	0.97
POPC/SM/Chol (1:1:1)	6	0.025	0.98
	8	0.045	0.98

Thus, the quantitative analysis above suggests that POPC/SM (1:1) LUV permeabilization mainly involves pores of defined size (six to eight monomers), whereas permeabilization of POPC and POPC/POPG (1:1) LUV probably obeys different mechanisms (see Refs. [4–6]), or insertion of the peptide into these membranes poses another barrier for pore formation. A factor that might be at the origin of SM effect could be the reduction in surface-aggregation reversibility (Table 1).

In Fig. 2A, we show the ability of melittin to induce leakage of contents from vesicles composed of POPC mixed with SM at various mole ratios. Melittin showed higher leakage efficiency upon increasing the SM content of vesicles. When the analog *N*-oleoyl SM substituted for bovine brain-SM in POPC/SM (1:1) LUV composition, the ability of melittin to induce leakage was reduced almost to the level detected in pure POPC. *N*-acyl unsaturation has been shown to interfere with SM ability to induce formation of ordered lipid domains [21]. Thus, it seems that leakage enhancement observed in the presence of SM is not due to the existence of stereospecific peptide–sphingolipid interactions but is rather related to the ability of natural SM to mediate lateral segregation into distinct lipid phases. This possibility was further tested. In PC/SM binary mixtures, s_o gel-phase formation starts when SM reaches 25–30 mol% [22,23]. Data displayed in panel 2B demonstrate that the threshold for SM-induced leakage stimulation and aggregation irreversibility in the binary mixtures roughly corresponded to above SM ratios. Importantly, as shown in panel 2C, leakage induced by the peptide was reduced to the levels measured in pure POPC by heating the samples above the chain melting temperature (T_m) of pure SM ($>37^\circ\text{C}$). This significant inhibitory effect of temperature was not observed with pure POPC, at least in the range of temperatures studied in Fig. 2B (data not shown). Thus, under conditions disrupting gel-phase SM-rich domains in the POPC/SM binary mixture, the leakage process was reduced close to the levels observed in pure POPC. However, it should be added that for pure POPC vesicles at a 1:100 peptide-to-lipid mole ratio, the final extent of leakage drops

from 92% at 20°C to 77% at 50°C , despite an expected increase in the fraction of peptide bound. According to the pore model [10,18], the degree of reversibility of surface aggregation of the peptide is expected to increase with temperature, that is, the parameter K_s and the final extents should decrease. The decrease in the final extents of peptide-induced leakage with temperature was previously observed for the peptide pardaxin [18] and for the peptide

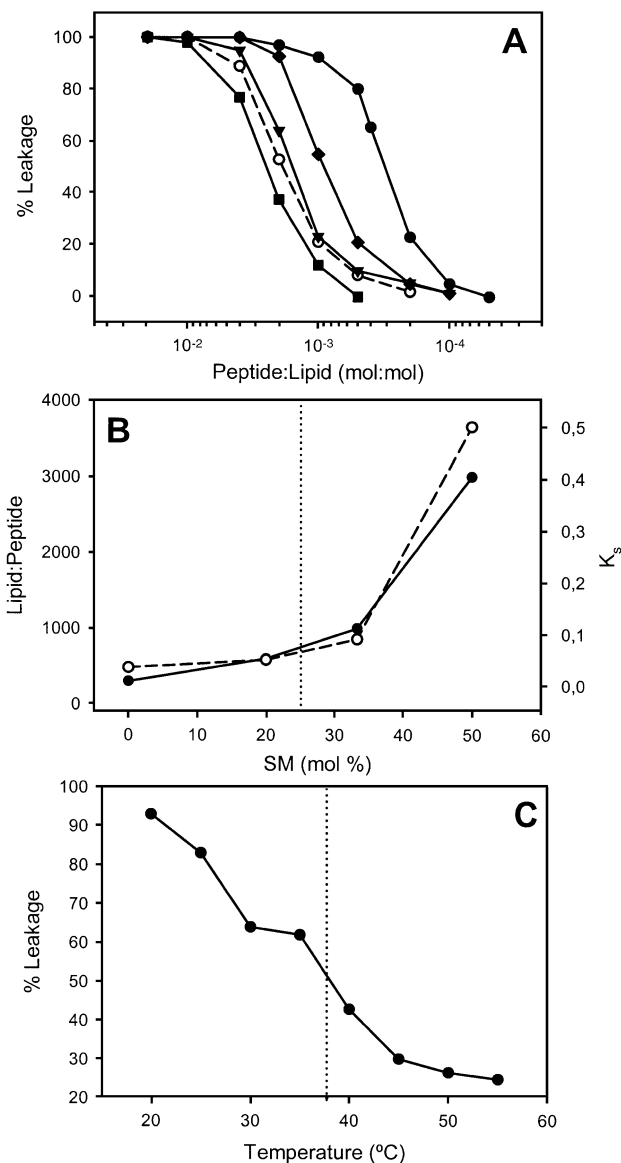


Fig. 2. Effects of SM on melittin-induced LUV permeabilization. (A) Final extents of leakage (percentage after 30 min) in POPC (squares), POPC/SM (4:1) (inverted triangles), POPC/SM (2:1) (diamonds), POPC/SM (1:1) (filled circles) and POPC/*N*-oleoyl SM (1:1) (empty circles) as a function of peptide-to-lipid mole ratio. (B) Surface aggregation constants (K_s) (empty circles) and lipid-to-peptide mole ratios required in membranes to induce 50% of vesicular content leakage (filled circles), plotted as a function of the SM mol% present in the binary mixtures. The dotted line begins at 25 mol%. (C) Effect of temperature on the melittin-induced leakage in POPC/SM (1:1) LUV (peptide-to-lipid ratio 1:250). The dotted line indicates the T_m of SM. Lipid concentration was 100 μM in all cases.

GALA (Nicol et al., unpublished). This peculiar temperature dependence of leakage due to pore formation by aggregating peptide molecules is in contrast to leakage due to enhanced permeability observed in liposomes and cells.

The inclusion of Chol in POPC/SM membranes has been shown to induce the formation of laterally segregated SPM/Chol-rich liquid-ordered (l_o) phases that coexist with liquid-disordered (l_d) phases [22,24–27]. Thus, we also tested whether coexistence of these two phases in the ternary mixture enhanced melittin-induced leakage of LUV. Experimental and calculated leakage data in Fig. 3 and Table 1 suggest that melittin was also able to assemble hexameric–octameric pores in POPC/SM/Chol (1:1:1, mole ratio) mixtures. However, in comparison to the binary mixture, the presence of Chol reduced by an order of magnitude the surface aggregation constants, a fact consisting with a higher level of peptide aggregation reversibility in these samples.

The previous analyses of leakage results according to hexameric–octameric pore models suggest that SM effects could arise from the enhancement of melittin clustering in the bilayer under conditions allowing for lipid phase coexistence. However, we wanted to test whether differences in the insertion capacity of melittin in the different mixtures might also explain SM effect. We studied melittin insertion by means of the lipid monolayer technique (Fig. 4). Comparable exclusion pressures, π_{ex} (i.e., initial surface pressures, π , at which $\Delta\pi=0$ after injection of the peptide into the subphase) were observed for pure POPC monolayers (37.6 mN m^{-1}) and the SM-containing POPC/SM (1:1) (35.2 mN m^{-1}) and POPC/SM/Chol (1:1:1) (33.0 mN m^{-1}) mixtures. The measured π_{ex} values were all above lateral pressures postulated to arise from the lipid packing densities existing in biological membranes ($\pi_{\text{ex}} \geq 30 \text{ mN m}^{-1}$, [28]). These data confirm that the presence of SM did not enhance

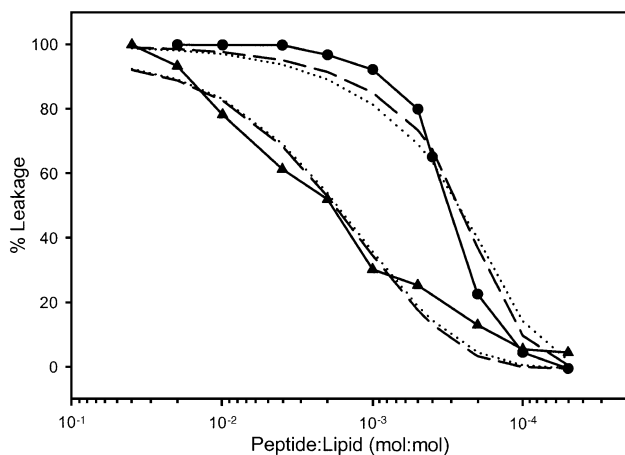


Fig. 3. Effects of cholesterol on melittin-induced permeabilization of POPC/SM LUV. Final extents of leakage (percentage after 30 min) in POPC/SM (1:1) (circles) and POPC/SM/Chol (1:1:1) (triangles) as a function of peptide-to-lipid mole ratio. Lipid concentration was $100 \mu\text{M}$. The curves correspond to the predicted values according to a pore model, calculated for $M=6$ (dashed) or $M=8$ (dotted).

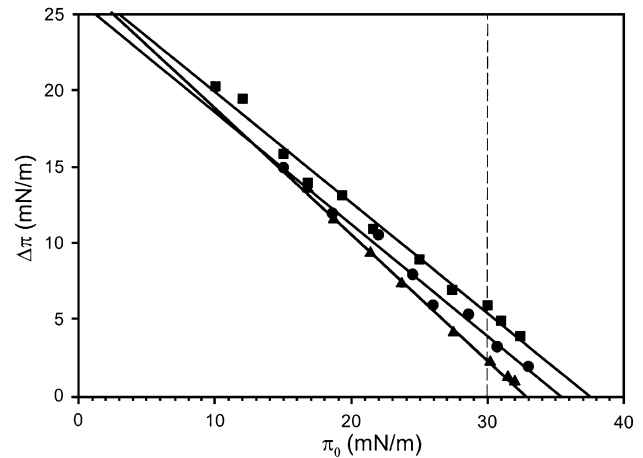


Fig. 4. Penetration of melittin into lipid monolayers. Maximum increase in surface pressure upon injection in the subphase of peptide ($0.14 \mu\text{M}$), measured as a function of the initial pressure of the phospholipid monolayer. Squares: POPC; circles: POPC/SM (1:1); triangles: POPC/SM/Chol (1:1:1). The dotted line begins at 30 mN m^{-1} .

the capacity of melittin to penetrate into the lipid monolayers.

The presence of SM did not alter the ability of melittin to partition from the aqueous phase into vesicles (Fig. 5). Following previous estimations [29,30], in our pore-model calculations, we assumed that melittin associated with neutral vesicles according to a molar fraction partition coefficient (K_x) of 10^6 . Data displayed in Fig. 5 indicate that the shifts in the maximum Trp emission upon titration with increasing lipid concentrations were comparable in POPC and POPC/SM (1:1) vesicles, and therefore consistent with a similar degree of peptide association. Moreover,

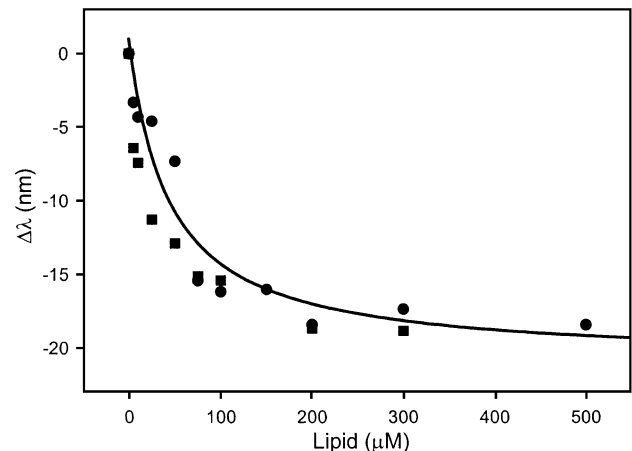


Fig. 5. Partitioning of melittin into POPC (squares) and POPC/SM (1:1) (circles) LUV. The wavelength shift of Trp emission was measured at increasing lipid concentrations as in Ref. [36]. Corrected spectra were recorded in a Perkin Elmer MPF-66 spectrofluorimeter with excitation set at 280 nm and 5-nm slits. The signal was further corrected for dilution and inner filter effects as described in Ref. [30] using the soluble Trp analog NATA which does not partition into membranes. The solid line fits to a partitioning isotherm with a K_x value of 10^6 .

both partitioning curves fitted quite well at K_x value of 10^6 . We may conclude that leakage assays in this study involving neutral vesicles (Figs. 1–3) were performed at comparable melittin doses in the membrane. On the other hand, partitioning into negatively charged vesicles has been shown to be several orders of magnitude higher than into electrically neutral ones [1,5]. Therefore, for the case of cationic melittin interacting with negatively charged POPC/POPG (1:1) vesicles (Fig. 1), quantitative partitioning was considered to occur at the 100 μ M lipid concentration used in the leakage assays. Thus, the remarkable differences detected in leakage efficiency (Fig. 1) cannot be explained on the basis of hypothetical differences in melittin ability to partition into membranes of different compositions.

4. Discussion

SM is a suitable candidate to modulate the toxic action of melittin upon its interaction with the erythrocyte plasma membrane. The distribution of lipids in this natural target membrane of melittin is highly asymmetric [31,32]. In the human erythrocyte, approximately equimolar amounts of PC and SM are predominantly found at the external membrane monolayer ($\sim 75\%$ and $\sim 80\%$ of total, respectively). Thus, zwitterionic choline-based phospholipids together with Chol are the principal lipid components of the membrane outer leaflet. Nonetheless and despite a compelling study of the interaction of melittin with model membranes, the effects of SM on its ability to permeabilize membranes via pore formation have been largely unknown. To our knowledge, only a previous report by Pott et al. [9] addressed the action of melittin on SM membranes. However, that study focused on the effects exerted by high doses of the peptide in pure SM membranes, and those authors particularly explored toxin-induced lipid polymorphism. In addition to that compelling study, Matsuzaki et al. [33] had previously reported that higher doses of melittin were required to permeabilize phosphatidylserine/SM (2:1 mole ratio) than pure POPC vesicles. In contrast, our work reveals that SM may stimulate melittin pore formation in electrically neutral bilayers.

The presence of SM did not increase the ability of melittin to penetrate into lipid monolayers or to partition into lipid bilayers. Size-distribution determinations by quasielastic light scattering in melittin-permeabilized LUV samples demonstrated that vesicle morphology was seemingly unaffected under our experimental conditions (data not shown). However, according to our data, melittin-induced leakage started in POPC/SM (1:1) vesicles at doses approximately 10 times lower than those required in pure POPC (Fig. 1). Moreover, a pore model gave a reasonable fit to the leakage results of POPC/SM (1:1) vesicles for pore sizes of $M=8$ and $M=6$. Increasing SM content in the membrane resulted in better fits to the hexameric–octameric pore model and enhancement of the surface aggregation constant (Table 1). Thus, the presence of SM enhanced peptide clustering and subsequent hexameric–octameric pore formation through the decrease of surface aggregation reversibility. In addition, the *N*-oleoyl SM analog could not sustain the stimulatory effect (Fig. 2). This fact, together with the effect exerted by temperature and SM content, suggest that lipid-phase coexistence plays a major role in SM-mediated leakage enhancement.

Of particular interest is the effect of Chol on hexameric–octameric melittin pore formation. Chol was known to inhibit the lysis of DPPC bilayers when melittin was incorporated at high doses below the T_m [8]. It was proposed that the tight lipid packing induced by the presence of Chol prevented the penetration of melittin into the bilayer [8]. In agreement with what had been described for the amphipathic peptide GALA [19], we found that the presence of Chol resulted in reduced efficiency of melittin-pore formation, because of an increased reversibility of peptide aggregation in membranes. Remarkably, the leakage data still fitted optimally to a hexameric–octameric peptide model (Fig. 3), indicating that the minimum number of peptides required to permeabilize a single vesicle did not change by the presence of Chol.

In summary, we may distinguish three different situations in electrically neutral membranes that depend on composition and lateral segregation of lipids (Fig. 6). Monomeric melittin is interfacial at low concentrations in membranes [2]. Thus, at low doses, in fluid (l_d) electrically neutral POPC bilayers, the preferred state of melittin is that of

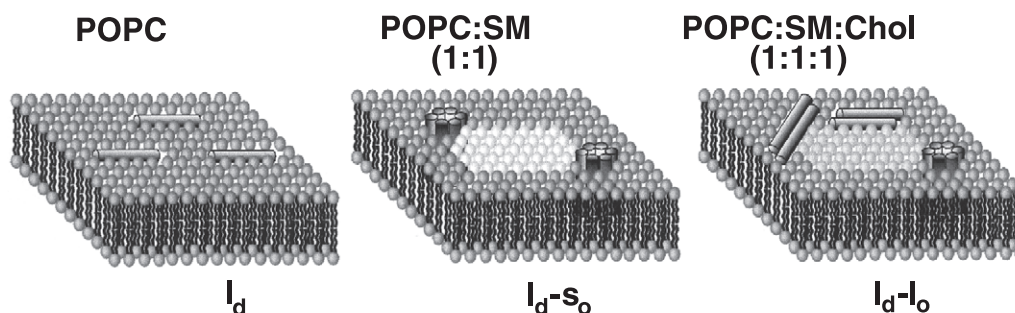


Fig. 6. Models for the preferred states of melittin (cylinders) at low concentrations in electrically neutral bilayers (see text for details). White, pale gray and dark gray lipid head-groups correspond to solid (s_o), liquid-ordered (l_o) and liquid-disordered (l_d) lipid phases, respectively.

surface-bound monomers arranged parallel to the membrane plane (left panel in Fig. 6). Coexistence of l_d and s_o phases in POPC/SM mixtures stimulates the irreversible assembly of discrete transmembrane pores (middle panel in Fig. 6). It has been postulated that dimerization is a rate-limiting step for melittin-induced leakage under some conditions (Ref. [34] and references therein). In-plane lipid heterogeneity has been related to the induction of lateral segregation of proteins [12–14]. Thus, it is possible that local accumulation of melittin monomers may be promoted by lipid phase coexistence as well. In addition, mismatch zones between gel-like condensed and fluid-disordered phases might provide a suitable environment for peptides to self-associate [27]. In the ternary POPC/SM/Chol mixture, l_o and l_d fluid phases coexist [25,27]. Therefore, it is likely that dimer formation is also promoted in this system by similar mechanisms. In this situation, the pore building blocks would be on standby at the interface, restrained in their capacity to translocate across the bilayer and assemble higher order complexes (right panel in Fig. 6). This fact is reflected in our pore model as a decrease in the surface aggregation constant (Table 1).

We have recently shown that membrane proximal regions in fusogenic viral proteins are amphipathic helices, associate with raft-type lipids and induce membrane perturbations [27,35]. It has been hypothesized that these sequences might play an active role in perturbing apposed membranes during fusion. It is tempting to speculate that modulation of the ability to damage bilayer architecture by lateral heterogeneity represents an adaptative mechanism shared by lytic sequences of diverse origin. We anticipate that this lipid-mediated regulatory mechanism may have wider implications for the toxic action of many relevant membrane-interacting peptides.

Acknowledgements

This work was supported by MCYT (Grant EET 2001/1954), the Basque Government (PI-1999-7) and the University of the Basque Country (UPV-13552/2001).

References

- [1] C.E. Dempsey, *Biochim. Biophys. Acta* 1031 (1990) 143–161.
- [2] K. Hristova, S.H. Dempsey, S.H. White, *Biophys. J.* 80 (2001) 801–811.
- [3] H. Vogel, F. Jähnig, *Biophys. J.* 50 (1986) 573–582.
- [4] A.S. Ladokhin, M.E. Selsted, S.H. White, *Biophys. J.* 72 (1997) 1762–1766.
- [5] A.S. Ladokhin, S.H. White, *Biochim. Biophys. Acta* 1514 (2001) 253–260.
- [6] T. Benachir, M. Lafleur, *Biochim. Biophys. Acta* 1235 (1995) 452–460.
- [7] J. Dufourcq, J. Faucon, G. Fourche, J. Dasseux, M. Le Maire, T. Gulik-Krzywicki, *Biochim. Biophys. Acta* 859 (1986) 33–48.
- [8] M. Monette, M. van Calsteren, M. Lafleur, *Biochim. Biophys. Acta* 1149 (1993) 319–328.
- [9] T. Pott, M. Paternostre, E.J. Dufourcq, *Eur. Biophys. J.* 27 (1998) 237–245.
- [10] S. Nir, J.L. Nieva, *Prog. Lipid Res.* 39 (2000) 181–206.
- [11] R.A. Parente, S. Nir, F.C. Szoka Jr., *Biochemistry* 29 (1990) 8720–8728.
- [12] A. Rietveld, K. Simons, *Biochim. Biophys. Acta* 1376 (1998) 467–479.
- [13] D.A. Brown, E. London, *J. Membr. Biol.* 164 (1998) 103–114.
- [14] D.A. Brown, E. London, *J. Biol. Chem.* 275 (2000) 17221–17224.
- [15] M.J. Hope, M.B. Bally, G. Webb, P.R. Cullis, *Biochim. Biophys. Acta* 812 (1985) 55–65.
- [16] C.S.F. Böttcher, C.M. van Gent, C. Fries, *Anal. Chim. Acta* 24 (1961) 203–204.
- [17] H. Ellens, J. Bentz, F.C. Szoka, *Biochemistry* 24 (1985) 3099–3106.
- [18] D. Rapaport, R. Peled, S. Nir, Y. Shai, *Biophys. J.* 70 (1996) 2503–2512.
- [19] F. Nicol, S. Nir, F.C. Szoka Jr., *Biophys. J.* 71 (1996) 3288–3301.
- [20] J.L. Nieva, S. Nir, A. Muga, F.M. Goñi, J. Wilschut, *Biochemistry* 33 (1994) 3201–3209.
- [21] B. Waarts, R. Bittman, J. Wilschut, *J. Biol. Chem.* 277 (2002) 38141–38147.
- [22] S.N. Ahmed, D.A. Brown, E. London, *Biochemistry* 36 (1997) 10944–10953.
- [23] M.P. Veiga, F.M. Goñi, A. Alonso, D. Marsh, *Biochemistry* 39 (2000) 9876–9883.
- [24] R.J. Schroeder, S.N. Ahmed, Y. Zhu, E. London, D.A. Brown, *J. Biol. Chem.* 273 (1998) 1150–1157.
- [25] A.U. Dietrich, C. Dietrich, L.A. Bagatolli, Z.N. Volovyyk, N.L. Thompson, M. Levi, K. Jacobson, E. Gratton, *Biophys. J.* 80 (2001) 1417–1428.
- [26] M.P. Veiga, J.L.R. Arrondo, F.M. Goñi, A. Alonso, D. Marsh, *Biochemistry* 40 (2001) 2614–2622.
- [27] A. Sáez-Cirión, S. Nir, M. Lorizate, A. Agirre, A. Cruz, J. Pérez-Gil, J.L. Nieva, *J. Biol. Chem.* 277 (2002) 21776–21785.
- [28] D. Marsh, *Biochim. Biophys. Acta* 1286 (1996) 183–223.
- [29] A.S. Ladokhin, S.H. White, *J. Mol. Biol.* 285 (1999) 1363–1369.
- [30] S. White, W.C. Wimley, A.S. Ladokhin, K. Hristova, *Methods Enzymol.* 295 (1998) 62–87.
- [31] M.S. Bretscher, *Science* 181 (1973) 622–629.
- [32] J. Rothman, J. Lenard, *Science* 195 (1977) 743–753.
- [33] K. Matsuzaki, K. Sugishita, N. Fuji, K. Miyajima, *Biochemistry* 34 (1995) 3423–3429.
- [34] J. Takei, A. Remenyi, C.E. Dempsey, *FEBS Lett.* 442 (1999) 11–14.
- [35] A. Sáez-Cirión, M.J. Gómara, A. Agirre, J.L. Nieva, *FEBS Lett.* 533 (2002) 47–53.
- [36] J. Dufourcq, J. Faucon, *Biochim. Biophys. Acta* 467 (1977) 1–11.